

The Conformational Changes of the Fungal Lipase from *Humicola lanuginosa* Induced by the Formation of Bile Salt and Mixed Micelles

A. Stobiecka¹

Received August 7, 1998; revised January 6, 1999; accepted January 7, 1999

The effect of sodium taurodeoxycholate and a mixture of sodium taurodeoxycholate/phosphatidylcholine on the activation of fungal lipase from *Humicola lanuginosa* (HLL) was investigated by monitoring the specific activity and the changes in intrinsic protein fluorescence. A large increase in the inactivation rate was observed at about the critical micellar concentration of bile salt. On the contrary, a high activation of lipase was achieved by the presence of mixed micelles. Steady-state fluorescence quenching measurements were performed to resolve the fluorescence contribution of W89 residue in emission of four-tryptophan-containing HLL lipase. The W89 residue is located in the "lid" helix which participates in interfacial activation of the enzyme. The assignment of W89 residue was confirmed by use of the W89F mutant and inhibited form of lipase. The FQRS (fluorescence quenching resolved spectra) method was used to decompose the total emission spectrum of HLL lipase. The FQRS results show that the fluorescence of the W89 residue is similar in inhibited and inactivated HLL lipase and exhibits a maximum of emission at about 345 ± 1 nm ($\lambda_{\text{ex}} = 295$ nm). In the mixed micelle solution the fluorescence of the W89 residue may be resolved into two components, with fluorescence maxima at 337 and 347 nm, respectively ($\lambda_{\text{ex}} = 295$ nm). It is concluded that HLL lipase undergoes a conformational transition upon specific interactions with both anionic and mixed micelles, resulting in a change in the microenvironment of the W89 residue.

KEY WORDS: *Humicola lanuginosa* lipase; micelles; lid.

INTRODUCTION

The fungal *Humicola lanuginosa* lipase belongs to a family of neutral lipases (acylglycerol acylhydrolases; EC 3.1.1.3) which preferentially hydrolyze fatty acids from the sn1 and sn3 positions of triglycerides. X-ray crystallographic studies have determined the 3-D structure of HLL lipase both in the native form [1] and complexed with inhibitors [2,3]. The results obtained from these investigations indicate that the molecular architecture and catalytic mechanism of the HLL lipase show

features similar to those of related enzymes [4–12]. The fungal acylhydrolase is a single-domain protein (MW = 30,000) built on eight central, twisted parallel β -sheet backbones connected by α -helices. The active site is composed of a Ser146–His258–Asp201 residue, reminiscent of the catalytic triad of serine proteases [13]. In the native (i.e., nonbound) enzyme, the active site is blocked by a short amphipathic α -helix, also called the "lid" or "flap." When complexed with inhibitors (or substrate analogues), the "lid" helix is displaced to one side, thereby exposing the catalytic triad. At the same time the nonpolar surface around the active site is enlarged. It was postulated that this conformational change is intimately related to the phenomenon of interfacial activation [14].

¹ Institute of General Food Chemistry, Technical University, Stefanowskiego 4/10 90-924, Łódź, Poland. e-mail: astobiec@snack.p.lodz.pl

The HLL lipase contains 4 tryptophans, 10 tyrosines, and 15 phenylalanines per molecule. Tryptophan residues, W89, W117, W221, and W260, are located in different regions of the protein. Significantly, the W89 residue is incorporated within a flexible "lid" helix which covers the active center under aqueous conditions [1]. It has been demonstrated experimentally that the W89 is essential for enzyme activity [15,16]. The results of X-ray studies of HLL–diethylphosphate and HLL–dodecylethylphosphate complexes, together with the molecular dynamics simulations [2], indicated a high mobility of the W89 side chain during interfacial activation.

The purpose of the present work was to investigate the structural changes of HLL lipase induced by interactions with both bile salt and mixed micelles. The intrinsic fluorescence of the W89 residue, located in the "lid" region, has been used as a probe for the dynamics of protein. To determine the fluorescence contribution of the W89 residue, steady-state fluorescence experiments were performed for native (so-called "closed" form), inhibited (so-called "open" form), and mutated enzyme. In the latter case the W89 residue was replaced by phenylalanine. It should be stressed that the site-directed mutagenesis did not induce any substantial conformational changes in the protein structure [15].

EXPERIMENTAL

The high-purity, lyophilized samples of the native (cHLL), inhibited (oHLL), and mutated (W89F) forms of *Humicola lanuginosa* lipase were a generous gift from Novo Nordisk, A/S Bagsvaerd, Denmark. The inhibited form of lipase was obtained by complexing the enzyme protein with phenylmethylsulfonyl fluoride (PMSF).

The best commercially available research-grade chemicals were used and were supplied by Sigma. All measurements were performed at $25 \pm 1^\circ\text{C}$ in 0.05 M Tris/HCl buffer, pH 8.0, containing 0.1 M NaCl, prepared in twice-distilled water.

Activity Measurements

HLL lipase activity was assayed using *p*-nitrophenyl acetate (PNPA) as a substrate [17]. The assay mixture for measuring PNPA hydrolysis consisted of 0.5–2.5 mM sodium taurodeoxycholate (NaTDOC) or 2 mM sodium taurodeoxycholate and 1 mM phosphatidylcholine (1,2-didodecanoyl-*sn*-3-glycerophosphocholine; DLPC), 0.1 M NaCl, 50 mM Tris/HCl buffer, pH 8.0, 25 mM substrate, and 5.38 μM enzyme protein in a total volume of 2 ml. Release of *p*-nitrophenol was determined using a Zeiss

spectrophotometer, Model Specol 11, adjusted to 399 nm. Substrate blanks were run under identical conditions, with Tris/HCl buffer added in place of enzyme. Plots of product formation as a function of time over 10 min were linear, thus allowing a reliable determination of the reaction rate. The initial hydrolysis rate, v_e , was calculated using the equation

$$v_e = \left[\left(\frac{\Delta A}{\Delta t} \right)_e - \left(\frac{\Delta A}{\Delta t} \right)_s \right] \quad (1)$$

where A is the absorption measured at 399 nm, t is the time of reaction, and the subscripts e and s correspond to hydrolysis by the enzyme and spontaneous substrate hydrolysis, respectively. One unit of enzyme activity corresponds to the hydrolysis of 1 μmol of PNPA/min performed in Tris/HCl buffer containing 0.1 M NaCl, pH 8.0, at 25°C .

Fluorescence Quenching

Fluorescence quenching measurements were performed using a Perkin–Elmer LS 50B fluorimeter. At excitation wavelengths ranging from 295 to 305 nm, the excitation band width was set to 2.5 nm. The emission bandwidth ranged from 2.5 to 4 nm. The protein solutions had an initial absorbance at an excitation wavelength lower than 0.1. All solutions were measured without previous degassing, in equilibrium with atmospheric oxygen. Fluorescence quenching experiments were performed by adding the microliter amounts of iodide concentrated solution directly to the protein sample in the cuvette. KI solutions were freshly prepared before each measurement and contained a trace of sodium thiosulfate to retard I_3^- formation. The fluorescence quenching data were fitted to the Stern–Volmer equation:

$$\frac{F}{F_0} = \sum_{i=1}^n \frac{f_i}{(1 + K_i[Q])} \quad (2)$$

where F_0 and F are the fluorescence intensities in the absence and presence of the quencher concentration $[Q]$, K_i is the dynamic quenching constant, and f_i is the fractional contribution of the fluorescent component, i . To resolve the fluorescence spectra of lipase into quenchable and unquenchable components, the fluorescence quenching resolved spectra (FQRS) procedure of Stryjowski and Wasylewski [18] was used. Each analysis was performed for about 18 potassium iodide quenching data sets obtained over the wavelength region of 320–400 nm. The parameters of Eq. (2) were calculated with the iterative nonlinear least-squares method.

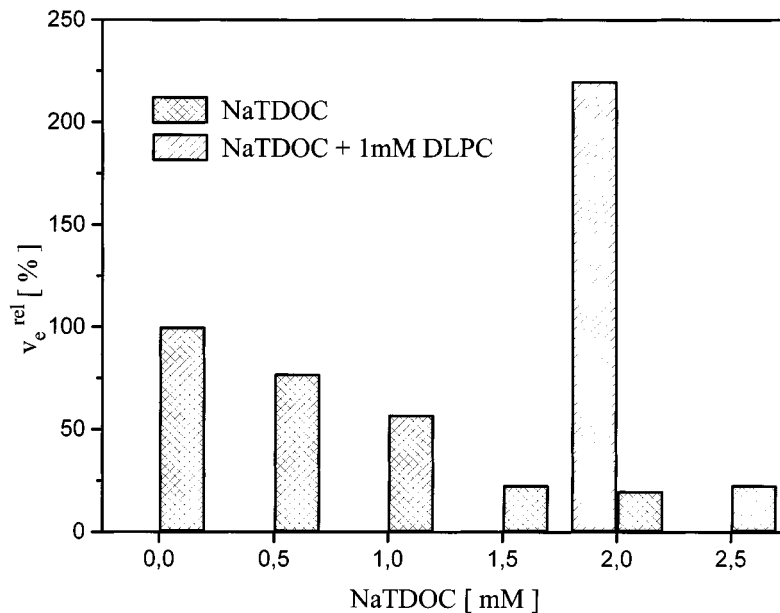


Fig. 1. Effect of sodium taurodeoxycholate (NaTDOC) and phosphatidylcholine (DLPC) on *p*-nitrophenyl acetate hydrolysis by *H. lanuginosa* lipase.

RESULTS AND DISCUSSION

Influence of NaTDOC and a Mixture of NaTDOC/DLPC on Hydrolysis of PNPA

In the absence of either bile salt (NaTDOC) or mixed micelles (NaTDOC/DLPC), solutions of PNPA are readily hydrolyzed by HLL lipase. Figure 1 shows that increasing the concentration of NaTDOC from 0.5 to 1.5 mM (values below the critical micelle concentration) caused a continuous decrease in the velocity of hydrolysis, v_e . Sodium taurodeoxycholate, at 2 mM (the cmc [19]), gives nearly complete inhibition of substrate hydrolysis. At the cmc, HLL lipase loses about 82% of its activity. If phosphatidylcholine (1 mM) is present in a 2 mM NaTDOC solution, the progressive loss of activity is halted and the initial rate of reaction becomes two times higher in comparison with control samples (i.e., without micelles). The essential result of these experiments is that the composition of the micelles significantly influenced the rate of PNPA hydrolysis (see Fig. 1). As shown in Table I, maximum enzyme activity was obtained in mixed micellar solutions with a weight ratio of cHLL/NaTDOC/DLPC of 1:6.5:3.9. With phosphatidylcholine and sodium taurodeoxycholate as micellar components, the rate of PNPA hydrolysis was increased 10-fold in comparison with a weight ratio of cHLL/NaTDOC of 1:6.5.

Quenching of Lipase Fluorescence by Iodide in the Absence and Presence of Micelles

The native, inhibited, and mutated forms of HLL lipase fluorescence quenching by KI were analyzed at pH 8.0. The HLL lipase is known to contain four tryptophan residues, W89, W117, W221, and W260 [20]. To resolve

Table I. Effect of the Chemical Composition of the Assay Mixture on PNPA Hydrolysis by *H. lanuginosa* Lipase

Component(s)	Weight ratio relative to lipase cHLL/NaTDOC/DLPC	Activity (μ U/mg protein)	Activation (%)
Lipase	None	39.4	0.0
Lipase + 0.5 mM NaTDOC	1:1.6:0	30.0	-23.9
Lipase + 1.0 mM NaTDOC	1:3.2:0	22.1	-43.9
Lipase + 1.5 mM NaTDOC	1:4.8:0	8.6	-78.2
Lipase + 2.0 mM NaTDOC	1:6.5:0	7.2	-81.7
Lipase + 2.5 mM NaTDOC	1:8.1:0	9.2	-76.7
Lipase + 2.0 mM NaTDOC + 1.0 mM DLPC	1:6.5:3.9	86.0	+118.3

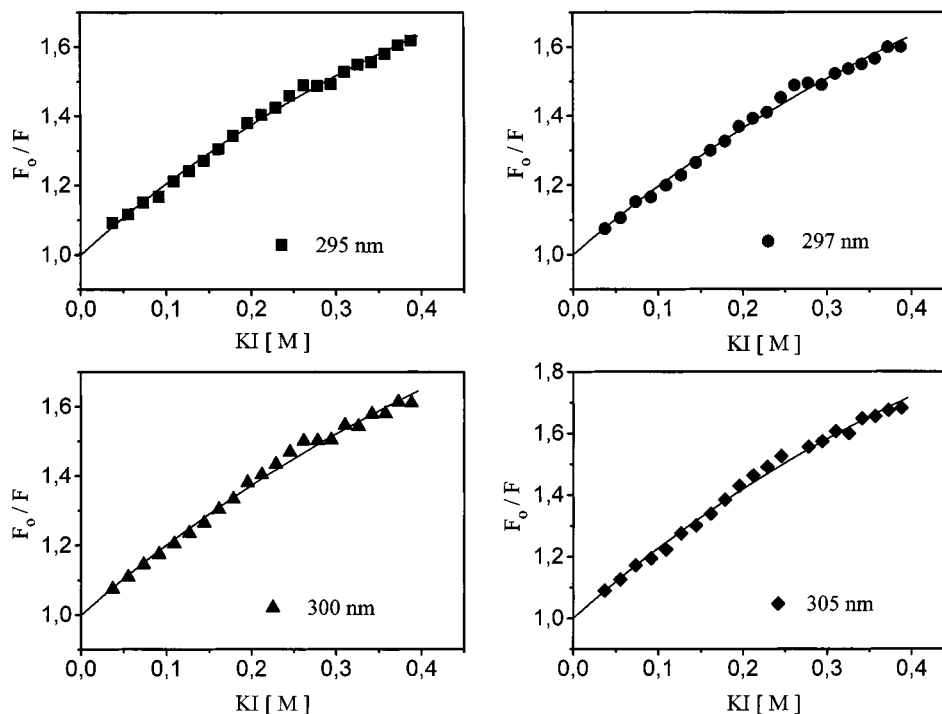


Fig. 2. Stern–Volmer plots for iodide quenching of native HLL lipase. The emission wavelengths were 340 nm in the excitation wavelength range 295–300 nm and 342 nm at $\lambda_{\text{ex}} = 305$ nm. The solid lines represent the best fits with the parameters presented in Table II.

the fluorescence emission spectra of the cHLL, oHLL, and W89F proteins into components, the fluorescence quenching data were analyzed at selected emission wavelengths according to the modified Stern–Volmer equation [Eq. (2)]. The fitting parameters were determined by minimizing the reduced χ^2 . Using the reduced χ^2 as well as the additional statistical goodness-of-fit criteria (i.e., the residual distribution of the experimental data and the lowest standard deviation of floating parameters: K_f and f_i), the best kinetic model was chosen.

Typical Stern–Volmer plots of fluorescence quenching of native and inhibited HLL lipase are shown in Figs. 2 and 3. The observed downward curvature of the Stern–Volmer plots for cHLL and oHLL protein implies the presence of two or more emitting components with different accessibilities to the quencher or it is caused by different combinations of dynamic and static quenching. On the contrary, the experimental data obtained for the W89F (Fig. 4) lipase indicate that tryptophan residues within the mutated enzyme are not available for iodide quenching. Thus, it can be assumed that under such conditions, only W89 tryptophyl fluorescence emission is quenched.

Considering the criteria mentioned above, the iodide-quenching data of the native and inhibited lipase appeared to be well described by the two-component

model, in which one class of tryptophans is quenched by KI, while the second one is totally inaccessible to the I^- . The relative intensities of the iodide-quenchable fractions (i.e., W89) obtained at the maximum of the total fluorescence spectrum of the cHLL and oHLL protein ($\lambda_{\text{max}} = 340$ nm, $\lambda_{\text{ex}} = 295$ nm) are about 69 and 56%, respectively. The quenching parameters together with the reduced χ^2 value and standard deviation values, calculated for cHLL and oHLL lipase, are presented in Table II. For example, the fluorescence-quenching resolved spectra (FQRS) of W89 within cHLL and oHLL protein when excited at 295 nm are presented in Fig. 5. The emission maxima of resolved spectra for the exposed (W89) and buried tryptophan residues are included in Table II. In the native form of HLL lipase, the W89 residue, characterized by $K_{\text{sv}} = 3.29 \text{ M}^{-1}$, exhibits emission at 343 nm ($\lambda_{\text{ex}} = 295$ nm). The inhibited form of the enzyme W89 residue emits fluorescence at 344 nm and the value of the dynamic constant is about one and half times higher ($K_{\text{sv}} = 4.23 \text{ M}^{-1}$) under the same experimental conditions. It may be assumed that the presence of lipase inhibitor covalently bound to the catalytic center causes the displacement of the flexible “lid” helix. Thus, it seems likely that the W89 residue within the inhibited, “open-lid” form of the enzyme becomes more exposed to the solvent in comparison with the native, “closed-

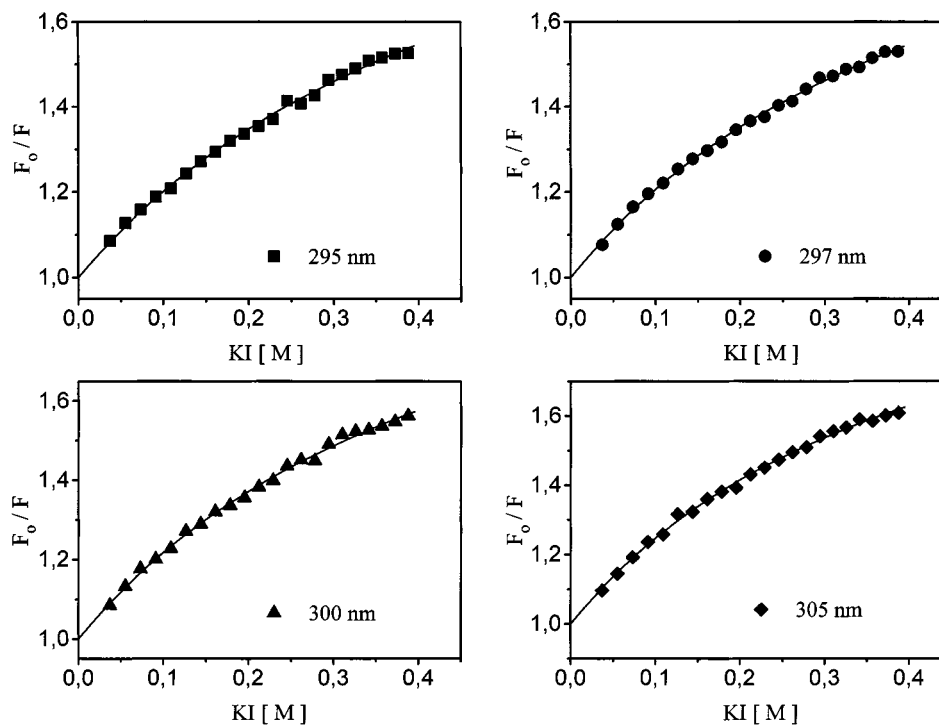


Fig. 3. Stern–Volmer plots for iodide quenching of inhibited HLL lipase. The emission wavelengths were 340 nm in the excitation wavelength range 295–305 nm. The best fits of the quenching data obtained for cHLL protein with the parameters given in Table II are presented as solid lines.

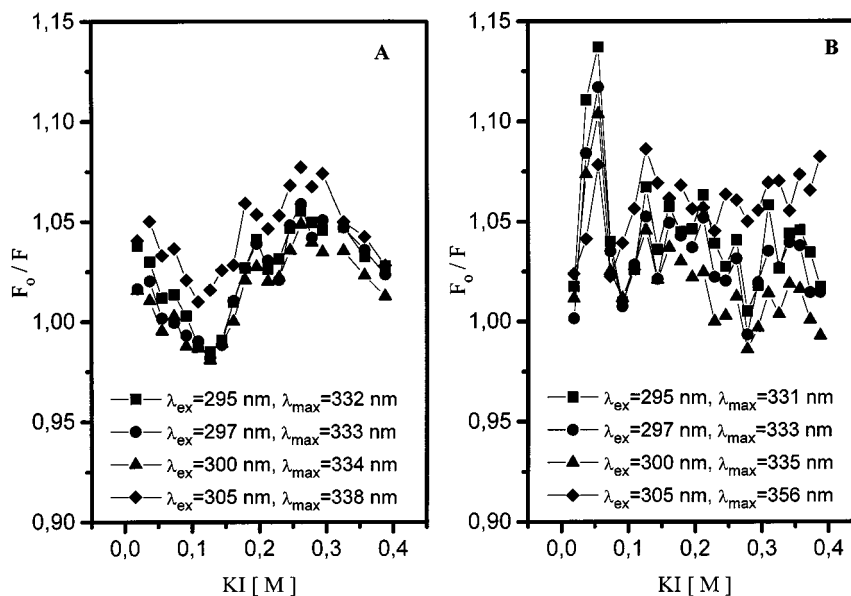


Fig. 4. Stern–Volmer plots of quenching of mutated HLL lipase by iodide in the absence (A) and presence (B) of mixed micelles.

lid” form of HLL lipase. This result is in reasonable agreement with the X-ray analysis of HLL–inhibitor complexes [2].

Using the same FQRS method, the fluorescence of cHLL lipase dissolved in solutions containing micelles was also decomposed into resolved spectra of tryptophan

Table II. Fluorescence Quenching Parameters for Native (cHLL) and Inhibited (oHLL) *H. lanuginosa* Lipase in 0.05 M Tris/HCl Buffer, pH 8.0^a

Lipase	λ_{ex} (nm)	K_1 (M^{-1})	f_1	K_2 (M^{-1})	f_2	χ^2	Resolved spectra	
							λ_{max1} (nm)	λ_{max2} (nm)
cHLL	295	0.00	0.31	3.29 (± 0.00)	0.69 (± 0.00)	0.751	333	343
	297	0.00	0.30	3.06 (± 0.00)	0.70 (± 0.00)	0.827	336	343
	300	0.00	0.28	3.04 (± 0.00)	0.72 (± 0.00)	0.788	336	344
	305	0.00	0.28	3.51 (± 0.00)	0.72 (± 0.00)	1.031	337	346
oHLL	295	0.00	0.44	4.23 (± 0.00)	0.56 (± 0.00)	0.306	335	344
	297	0.00	0.45	4.51 (± 0.00)	0.55 (± 0.00)	0.178	337	344
	300	0.00	0.44	4.65 (± 0.00)	0.56 (± 0.00)	0.312	337	345
	305	0.00	0.46	5.67 (± 0.00)	0.54 (± 0.00)	0.291	340	348

^a The emission was observed at the maximum of the fluorescence spectrum of proteins. The values in parentheses are the standard deviations of the parameters obtained.

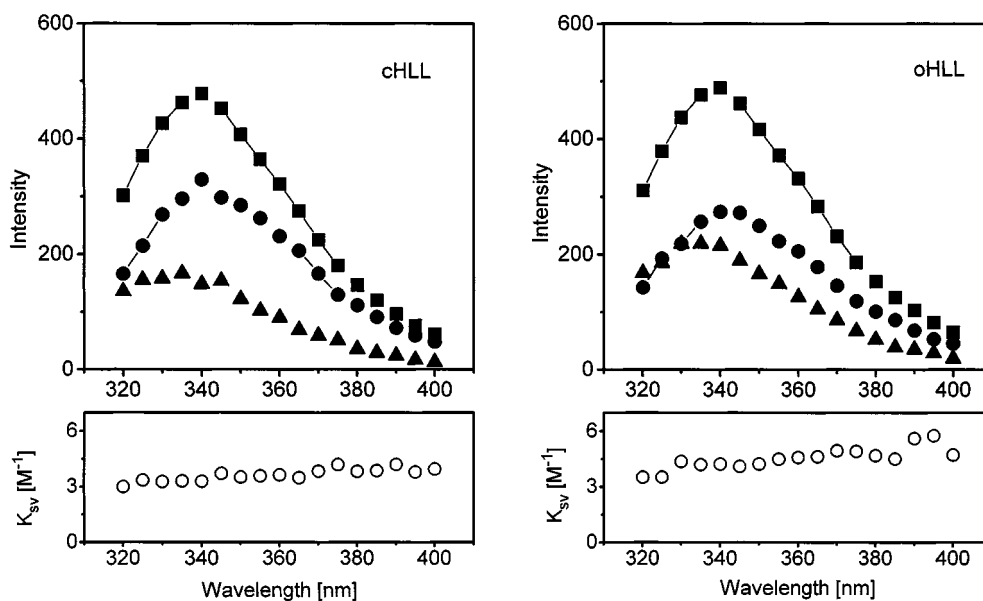


Fig. 5. Fluorescence quenching resolved spectra of native (cHLL) and inhibited (oHLL) *H. lanuginosa* lipase obtained with excitation at 295 nm, using potassium iodide as the quencher. (●) Quenchable component; (▲) unquenchable component; (■) total steady-state emission spectrum of protein. The lower panels show the Stern–Volmer constant dependence on the emission wavelength.

residues. In the case of anionic micellar solutions the best fits [Eq. (2)] were achieved with the two-class model of tryptophan residues: accessible to I^- and completely inaccessible to I^- . The fitting parameters are summarized

in Table III. The average fractional contributions of quenchable and unquenchable fractions of cHLL fluorescence at the excitation wavelengths 295–305 nm are equal to 53 and 47%, respectively. The dynamic quenching

Table III. Fluorescence Quenching Parameters for Native *H. lanuginosa* Lipase in Tris/HCl Buffer, pH 8.0, Containing Anionic and Mixed Micelles^a

Micellar component(s)	λ_{ex} (nm)	K_1 (M^{-1})	f_1	K_2 (M^{-1})	f_2	χ^2	Resolved spectra	
							λ_{max1} (nm)	λ_{max2} (nm)
NaTDOC	295	0.00	0.48	4.90 (± 0.00)	0.52 (± 0.00)	1.072	335	345
	297	0.00	0.47	5.02 (± 0.00)	0.53 (± 0.00)	0.656	336	346
	300	0.00	0.47	5.14 (± 0.00)	0.53 (± 0.00)	0.239	338	346
	305	0.00	0.46	5.41 (± 0.00)	0.54 (± 0.00)	0.253	337	348
NaTDOC/DLPC	295	0.64 (± 0.01)	0.70 (± 0.01)	6.24 (± 0.02)	0.30 (± 0.00)	0.569	337	347
	297	0.55 (± 0.03)	0.61 (± 0.02)	4.39 (± 0.03)	0.39 (± 0.01)	1.024	336	346
	300	0.44 (± 0.05)	0.51 (± 0.04)	3.66 (± 0.03)	0.49 (± 0.01)	1.129	338	346
	305	0.00	0.31	3.40 (± 0.00)	0.69 (± 0.00)	0.840	341	347

^a The emission was observed at the maximum of the fluorescence spectrum of protein. The values in parentheses are the standard deviations of the parameters obtained.

constant of the component which is exposed to the solvent has a value of $K_{\text{sv}} = 4.90 M^{-1}$ ($\lambda_{\text{ex}} = 295$ nm). This value and the relative intensity are similar to those found for the component quenched by iodide (i.e., W89) within the inhibited HLL lipase. The average maximum of fluorescence emission of the quenchable component equals 346 nm and the maximum of the second component equals 337 nm (see Table III and Fig. 6).

For the cHLL protein dissolved in buffer containing mixed micelles, the best fits [Eq. (2)] at the excitation wavelengths 295–300 nm were obtained with a two-class model in which both components are quenchable by KI. The fitting parameters are given in Table III. In the FQRS spectra presented in Fig. 7A, the less quenchable component, characterized by an iodide Stern–Volmer constant equal to $K_{\text{sv1}} = 0.64 M^{-1}$, is found to exhibit a maximum at 337 nm and to participate in 70% of the fluorescence emission ($\lambda_{\text{ex}} = 295$ nm). The second component, characterized by $K_{\text{sv2}} = 6.24 M^{-1}$, has a maximum at 347 nm and participates in about 30% of the total emission under the same conditions. The maxima of the resolved spectra for the two quenchable fractions are included in Table III. The steady-state iodide-quenching data of the W89F protein dissolved in Tris/HCl buffer containing mixed micelles show that three tryptophan residues, W117, W221, and W260, are not available for the quencher (Fig. 4). This result indicates that the presence of two iodide-quenchable components of cHLL lipase in solutions con-

taining mixed micelles can be related to the microheterogeneity of the W89 tryptophan environment.

CONCLUSION

The fluorescence quenching experiments show that the presence of anionic and mixed micellar solutions influenced the quenching of HLL lipase. These results suggest increased accessibility of the W89 residue within protein when dissolved in either a 2 mM sodium taurodeoxycholate or a 2 mM sodium taurodeoxycholate/1 mM phosphatidylcholine solution.

The loss of lipase activity caused by interactions with anionic micelles is accompanied by an increase in the Stern–Volmer constant calculated for the W89 residue. According to the FQRS results, the values of the dynamic constant and fractional contribution of the W89 residue within inhibited lipase are similar to those obtained for native HLL lipase in a 2 mM NaTDOC solution. On the other hand, the iodide-quenching experiments performed for cHLL protein in solutions containing mixed micelles suggest that the side chain of the W89 residue possesses a relatively higher mobility. Thus, the increased flexibility of the “lid” helix might be accompanied by activation of the HLL lipase observed in assay mixtures containing NaTDOC/DLPC micelles.

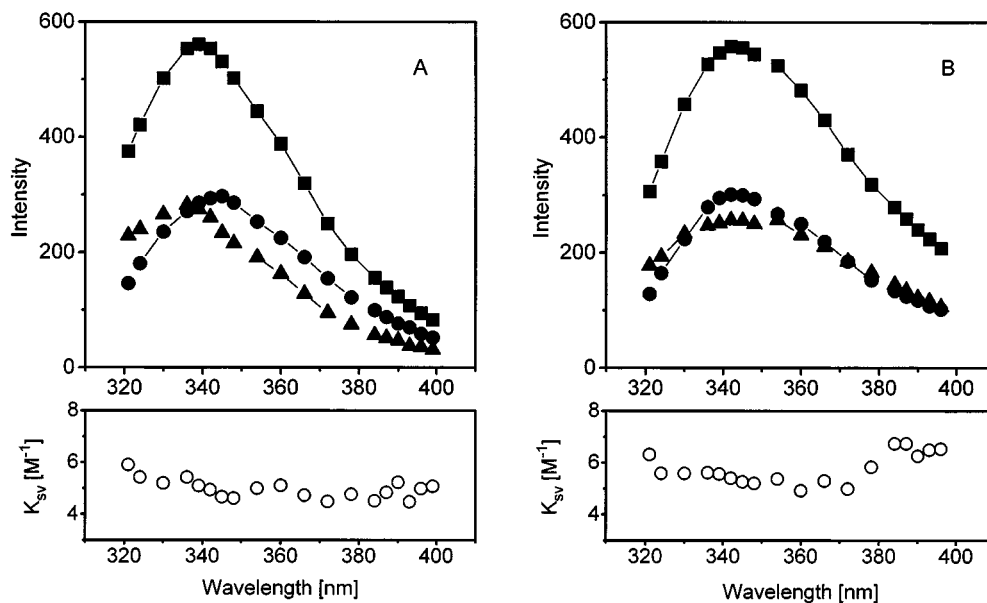


Fig. 6. Fluorescence quenching resolved spectra of native (cHLL) *H. lanuginosa* lipase obtained with excitation at 295 nm (A; $\lambda_{\max} = 339$ nm) and 305 nm (B; $\lambda_{\max} = 342$ nm), using potassium iodide as the quencher. Fluorescence was measured in 0.05 M Tris/HCl, pH 8.0, containing 2 mM NaTDOC. (●) Quenchable component; (▲) unquenchable component; (■) total steady-state emission spectrum of protein. The lower panels show the Stern–Volmer constant dependence on the emission wavelength.

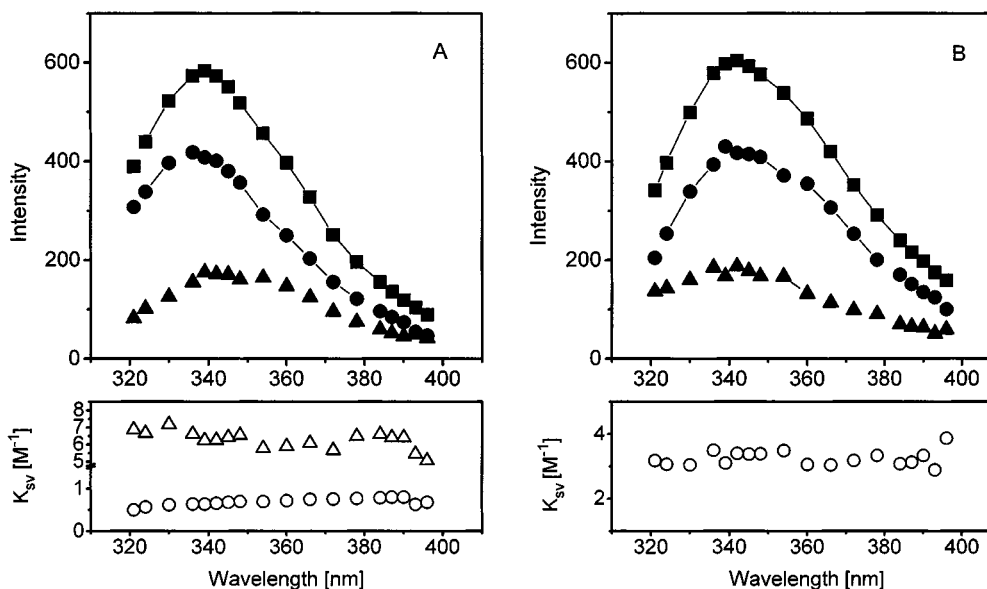


Fig. 7. Fluorescence quenching resolved spectra of native (cHLL) *H. lanuginosa* lipase obtained with excitation at 295 nm (A) and 305 nm (B), using potassium iodide as the quencher. Fluorescence was measured in 0.05 M Tris/HCl, pH 8.0, containing 2 mM NaTDOC/1 mM phosphatidylcholine. (A) (●) The blue component ($\lambda_{\max 1} = 337$ nm, $K_{sv} = 0.64$ M⁻¹); (▲) the red component ($\lambda_{\max 2} = 347$ nm; $K_{sv} = 6.24$ M⁻¹); (■) total steady-state emission spectrum of protein ($\lambda_{\max} = 339$ nm). (B) (▲) unquenchable component ($\lambda_{\max 1} = 341$ nm, $K_{sv} = 0.00$ M⁻¹); (●) quenchable component ($\lambda_{\max 2} = 347$ nm, $K_{sv} = 3.40$ M⁻¹); (■) total steady-state emission spectrum of protein ($\lambda_{\max} = 342$ nm). The lower panels show the Stern–Volmer constant dependence on the emission wavelength.

It might be assumed that the structure of HLL lipase in solutions containing mixed as well as bile salt micelles must differ substantially from the "closed" structure of native form of enzyme. Probably, the active open-"lid" conformation of HLL lipase is achieved only in the presence of mixed micelles. On the contrary, in PMSF-inhibited enzyme or in enzyme dissolved in buffer containing anionic micelles, the "lid" helix adopts an open conformation which is not suitable for PNPA hydrolysis. The results presented herein support the suggestion that the exact positioning of the "lid" must be crucial for efficient catalysis provided with HLL lipase.

ACKNOWLEDGMENTS

I wish to express my thanks to Novo Nordisk for the gift of *H. lanuginosa* samples. I am also very grateful to Prof. Zygmunt Wasylewski for supplying me with the FQRS computer program.

REFERENCES

1. U. Derewenda, L. Swenson, R. Green *et al.* (1994) *Protein Eng.* **7**, 551–557.
2. D. M. Lawson, A. M. Brzozowski, S. Rety *et al.* (1994) *Protein Eng.* **7**, 543–550.
3. A. M. Brzozowski (1993) *Acta Cryst.* **D49**, 352–354.
4. F. K. Winkler, A. D'Arcy, and W. Hunziker (1990) *Nature* **343**, 771–774.
5. H. Van Tilbeurgh, M. P. Egloff, Ch. Martinez *et al.* (1993) *Nature* **362**, 814–820.
6. L. Brady, A. M. Brzozowski, Z. S. Derewenda *et al.* (1990) *Nature* **343**, 767–770.
7. U. Derewenda, A. M. Brzozowski, D. M. Lawson, and Z. S. Derewenda (1992) *Biochemistry* **31**, 1532–1541.
8. A. M. Brzozowski, U. Derewenda, Z. S. Derewenda *et al.* (1991) *Nature* **351**, 491–494.
9. J. D. Schrag, and M. Cygler (1993) *J. Mol. Biol.* **230**, 575–591.
10. P. Grochulski, Y. Li, J. D. Schrag *et al.* (1993) *J. Biol. Chem.* **268**, 12843–12847.
11. P. Grochulski, Y. Li, J. D. Schrag, and M. Cygler (1994) *Prot. Sci.* **3**, 82–91.
12. J. Uppenberg, N. Ohrner, M. Norin *et al.* (1995) *Biochemistry* **34**, 16838–16851.
13. D. M. Lawson, A. M. Brzozowski, and G. G. Dodson (1992) *Curr. Biol.* **2**, 473–475.
14. P. Desnuelle, L. Sarda, and G. Ailhaud (1960) *Biochim. Biophys. Acta* **37**, 570–571.
15. M. Holmquist, I. G. Clausen, S. Patkar *et al.* (1995) *J. Prot. Chem.* **14**, 217–224.
16. M. Martinelle, M. Holmquist, I. G. Clausen *et al.* (1996) *Protein Eng.* **9**, 519–524.
17. C. Chapus, M. Semeriva, C. Bovier-Lapierre, and P. Desnuelle (1976) *Biochemistry* **15**, 4980–4987.
18. W. Stryjowski and Z. Wasylewski (1986) *Eur. J. Biochem.* **158**, 547–553.
19. A. Helenius, D. McCaslin, D. R. Fries, and C. Tanford (1976) *Methods Enzymol.* **56**, 734–749.
20. D. M. Lawson, A. M. Brzozowski, G. G. Dodson *et al.* (1994) in P. Woolley and S. B. Petersen (Eds.), *Lipases, Their Structure, Biochemistry and Application*, Cambridge University Press, Cambridge, pp. 77–94.